OPEN

Oncogene (2017), 1–13

www.nature.com/onc

ORIGINAL ARTICLE

CECR1-mediated cross talk between macrophages and vascular mural cells promotes neovascularization in malignant glioma

C Zhu[1,2,6], I Chrifi[3,6], D Mustafa[1], M van der Weiden[1], PJM Leenen[4], DJ Duncker[3], JM Kros[1,7] and C Cheng[3,5,7]

Glioblastomas (glioblastoma multiforme, GBM) are most malignant brain tumors characterized by profound vascularization. The activation of macrophages strongly contributes to tumor angiogenesis during GBM development. Previously, we showed that extracellular adenosine deaminase protein Cat Eye Syndrome Critical Region Protein 1 (CECR1) is highly expressed by M2-like macrophages in GBM where it defines macrophage M2 polarization and contributes to tumor expansion. In this study, the effect of CECR1 in macrophages on tumor angiogenesis was investigated. Immunohistochemical evaluation of GBM tissue samples showed that the expression of CECR1 correlates with microvascular density in the tumors, confirming data from the TCGA set. In a three-dimensional co-culture system consisting of human pericytes, human umbilical vein endothelial cells and THP1-derived macrophages, CECR1 knockdown by siRNA and CECR1 stimulation of macrophages inhibited and promoted new vessel formation, respectively. Loss and gain of function studies demonstrated that PDGFB mRNA and protein levels in macrophages are modulated by CECR1. The proangiogenic properties of CECR1 in macrophages were partially mediated via paracrine activation of pericytes by PDGFB–PDGFRβ signaling. CECR1–PDGFB–PDGFRβ cross-activation between macrophages and pericytes promoted pericyte migration, shown by transwell migration assay, and enhanced expression and deposition of periostin, a matrix component with proangiogenic properties. CECR1 function in (M2-like) macrophages mediates cross talk between macrophages and pericytes in GBM via paracrine PDGFB–PDGFRβ signaling, promoting pericyte recruitment and migration, and tumor angiogenesis. Therefore, CECR1 offers a new portent target for anti-angiogenic therapy in GBM via immune modulation.

Oncogene advance online publication, 22 May 2017; doi:10.1038/onc.2017.145

INTRODUCTION

Glioblastoma multiforme (GBM) represents the highest grade of glioma and carries a dismal prognosis of merely 12–15 months, even after current standard chemo-radiotherapy and tumor resection regimes.[1] Presently, our understanding of the exact mechanisms driving GBM pathogenesis remains limited and further research is essential for the design of more effective therapies. GBMs are highly vascularized tumors that are hallmarked by vascular hyper-proliferative capacity[2] and vast myeloid infiltration.[3]

So far, the therapeutic effects of anti-angiogenic regimes targeting VEGF were shown to be limited, due to rapid acquirement of resistance by the tumor cells.[4] It has been proposed that the drug resistance may be related to the activation of alternative angiogenic pathways such as FGF2-mediated and HIF1-independent mechanisms that bypass the need for VEGFA regulation of tumor angiogenesis.[5] In addition, the recruitment and activation of bone marrow-derived circulatory cells, including macrophages, could rescue tumor angiogenesis by secretion of these alternative proangiogenic factors.[6]

Previous studies have well established the involvement of resident macrophages (microglia) and infiltrated macrophages, also called glioma-associated macrophages (GAMs), in tumor angiogenesis of GBM.[7,8] Although GAMs can produce VEGFA, alternative mechanisms including GAMs-induced RAGE-,[9] CXCL2[10] - and IGFBP1[11]-mediated regulation of tumor angiogenesis, have also been demonstrated. In addition to regulating angiogenesis, GAMs actively promote glioma growth, migration and invasion,[12] and help maintain a glioma stem cell niche.[13] Furthermore, findings of clinical studies imply an important functional contribution of GAMs to the prognosis or recurrence of GBM.[3,8,14,15] Several studies pointed out that macrophages in GBMs mainly originated from major infiltrated myeloid cell populations[7,16,17] and not from resident microglia. A diminished population of $P2RY12^{+}$ cells (microglia cells) in GBMs was also detected in our previous study.[18] Macrophages are classically distinguished into M1 and M2 phenotypes. M1 macrophages are primarily associated with a pro-inflammatory state, whereas M2 macrophages are associated with immune modulation and wound healing. Compared with M1 macrophages, M2 macrophages have been shown to act proangiogenic, both *in vitro* and *in vivo*.[19–21]

[1]Department of Pathology, Erasmus Medical Center, Rotterdam, The Netherlands; [2]Department of Pediatric Neurosurgery, Shanghai Xinhua Hospital affiliated to School of Medicine, Shanghai Jiao Tong University, Shanghai, China; [3]Division of Experimental Cardiology, Department of Cardiology, Thoraxcenter, Erasmus Medical Center, Rotterdam, The Netherlands; [4]Department of Immunology, Erasmus Medical Center, Rotterdam, The Netherlands and [5]Department of Nephrology and Hypertension, DIGD, University Medical Center Utrecht, Utrecht, The Netherlands. Correspondence: Professor JM Kros, Department of Pathology, Erasmus Medical Center, Room Be 230c, Wytemaweg 80, PO Box 2040, 3015 CN, 3000 CA Rotterdam, The Netherlands.
E-mail: j.m.kros@erasmusmc.nl
[6]These authors contributed equally to this work.
[7]These authors contributed equally to this work.
Received 26 August 2016; revised 6 February 2017; accepted 4 April 2017

In line with these observations, recent studies have indicated that mainly tumor-associated macrophages with a M2-like phenotype can act as proangiogenic modulators, stimulating expansion of disorganized neovessels by, for example, paracrine release of PIGF[22] and CCL18.[23] In GBM, M2-like GAMs have been mainly described for their immune-suppressive and tumor-supportive function. As the majority of GAMs in GBM are known to have a M2-like phenotype, specific drug targeting of M2 macrophages could become a viable alternative therapy for the inhibition of tumor angiogenesis in GBM.[6]

Recently, the extracellular adenosine deaminase protein Cat Eye Syndrome Critical Region Protein 1 (CECR1) has been shown to regulate macrophage maturation. In previous studies , we demonstrated that CECR1 is consistently highly expressed by M2-type GAMs, particularly in high-grade glioma.[24] In line with the findings presented by Navon *et al*.[25] and Zhou and colleagues,[26] we could validate that CECR1 is an important promoter of GAM polarization towards M2-like macrophages. Our previous study also demonstrated that CECR1-mediated paracrine activation of M2-like GAMs directly affected the GBM cells, promoting tumor cell proliferation and migration. However, the effect of CECR1 regulation of GAMs on tumor angiogenesis remains to be investigated. Considering the important role that CECR1 has in M2-like macrophage polarization, and the general proangiogenic function of GAMs, we hypothesize that CECR1 contributes to the paracrine proangiogenic function of (M2-like) GAMs.

In the present study, we demonstrated that CECR1 expression correlated with microvascular density in GBM samples-based analysis. Using a well-validated three-dimensional (3D) co-culture system consisting of human pericytes, human umbilical vein endothelial cells (HUVECs) and THP1-derived macrophages, we further demonstrated that gain and loss of function of CECR1 activity in macrophages inhibited and promoted new vessel formation, respectively. Further investigation revealed that CECR1 modulated pericyte function (mainly migration), a process that was mediated by CECR1–PDGFB–PDGFRβ paracrine cross talk between macrophages and pericytes.

RESULTS

CECR1 levels correlate with microvascular density in human GBM

Immunohistochemical analysis of human GBM samples indicated strong CECR1 intensity in GBM samples with high microvascular density, as shown by CD31+ staining of vascular endothelium (Figure 1a). The high level of CECR1 coincided with a strong signal of CD204+ M2 macrophages. In contrast, regions in GBM samples with weak CECR1 immunostaining showed limited numbers of CD204+ cells, and low microvascular density (Figure 1a). This correlation between CECR1 and M2 macrophage markers (CD204, in addition to CD163) was further validated in the TCGA database (Supplementary Figure 1). Quantitative analysis using ImageJ software confirmed the data of this initial visual evaluation, with the mean percentage of CD31+ area per image field per GBM sample being significantly higher in the group of samples with high versus low CECR1 levels (Figure 1b). Further analysis revealed a significant positive correlation between the CD31 and CECR1 in the collection of GBM samples (Figure 1c). These data were in line with the findings obtained by data mining in the TCGA data set: significant positive correlations were identified between PECAM1 (endothelial cell marker), Endoglin (endothelial (progenitor) cell marker) and CECR1 expression in a set of 166 samples (Figures 1d and f). The findings were validated in a second TCGA GBM set[27] of 154 GBM samples (Figures 1e and g). Taken together, these observations indicate that high CECR1 levels in GBM relate to high microvascular density and the presence of CD204+ M2 macrophages.

CECR1 promotes the proangiogenic paracrine action of M2 macrophages

Previously, we have identified M2-like macrophages as the main cell type in GBM to produce high levels of CECR1. We also showed that CECR1 promotes M0 to M2 macrophage polarization and determined M2 paracrine activity. Here we investigated the function of CECR1 in macrophage-mediated angiogenesis in a GBM-like environment. Angiogenesis was assessed in a 3D co-culture assay consisting of a collagen matrix in which GFP-labeled HUVECs directly interact with dsRed-labeled human-derived pericytes. This complex system mimics the complete sequence of events in microvasculature formation, allowing us to study vessel sprouting, vascular cell migration through a 3D matrix environment, multicellular vessel formation, lumenization, pericyte recruitment, perivascular coverage and microvascular stabilization, all within a 5-day time range. To assess CECR1 function in GAMs in a GBM environment, THP1 monocytic cells were maturated by stimulation with PMA for 48 h, before transfection with CECR1 targeting siRNA to obtain CECR1-silenced macrophages. These siCECR1 macrophages were further stimulated for 48 h with or without U87-derived medium to assess the effect of a GBM paracrine environment. To assess the paracrine effect of the modified macrophages on angiogenesis, the THP1-derived macrophages were harvested and seeded on top of the co-culture system (Figure 2a). Stimulation of the co-cultures with THP1 macrophages significantly increased microvascular density, as observed by quantitative analysis of the number of tubules, total tubule length and number of junctions at day 5 (Figures 2b, c and f). Successful siRNA-mediated knockdown CECR1 in THP1 macrophages, as validated by western blot and quantitative PCR (qPCR, Figure 2e), significantly reduced the response of the co-culture to the macrophages, as shown by a reduction in total tubule length compared with treatment with sisham and control macrophages. These effects were further amplified when the co-cultures were treated with THP1 macrophages stimulated with U87 supernatant during maturation, with CECR1-silenced+U87 supernatant-treated THP1 cells reducing the number of tubules and junctions and decreasing the total tubule length in the exposed co-cultures compared with the control groups (Figures 2d and f–h). In contrast, stimulation of co-cultures with THP1 macrophages that were stimulated with human recombinant CECR1 during maturation, showed a significant increase in all assessed vascular parameters (Supplementary Figures 2a and b), demonstrating a dose–response relation. In addition, stimulation with exogenous CECR1 during macrophage maturation induced a partial rescue of attenuated tube formation that was triggered by THP1 cells with CECR1 silencing (Supplementary Figure 3).

Our previous studies demonstrated that M2 macrophages were the main producers of CECR1 in GBM. Here we investigated whether the paracrine proangiogenic effects could be partially mediated by direct stimulation of vascular cells by CECR1. Indeed, stimulation of the co-cultures with recombinant CECR1 increased the number of junctions, tubules and total tubule length, demonstrating that vascular cells can be directly stimulated by CECR1 (Supplementary Figures 4a and b). Combined, these data indicate that CECR1 has an important role in regulating the proangiogenic function of macrophages.

PDGFB expression correlates with M2 GAMs and is enhanced by CECR1

To identify which particular known proangiogenic molecules are associated to the expression of CECR1, qPCR was carried out on nine well-recognized proangiogenic genes (PDGFB, VEGFA, ANGPT1, ANGPT2, MMP7, MMP9, VWF, IL8, Tie-2). QPCR analysis of macrophages showed that stimulation with recombinant human (rh)CECR1 significantly increased PDGFB in a dose-responsive manner (Figure 3b, Supplementary Figure 5). In

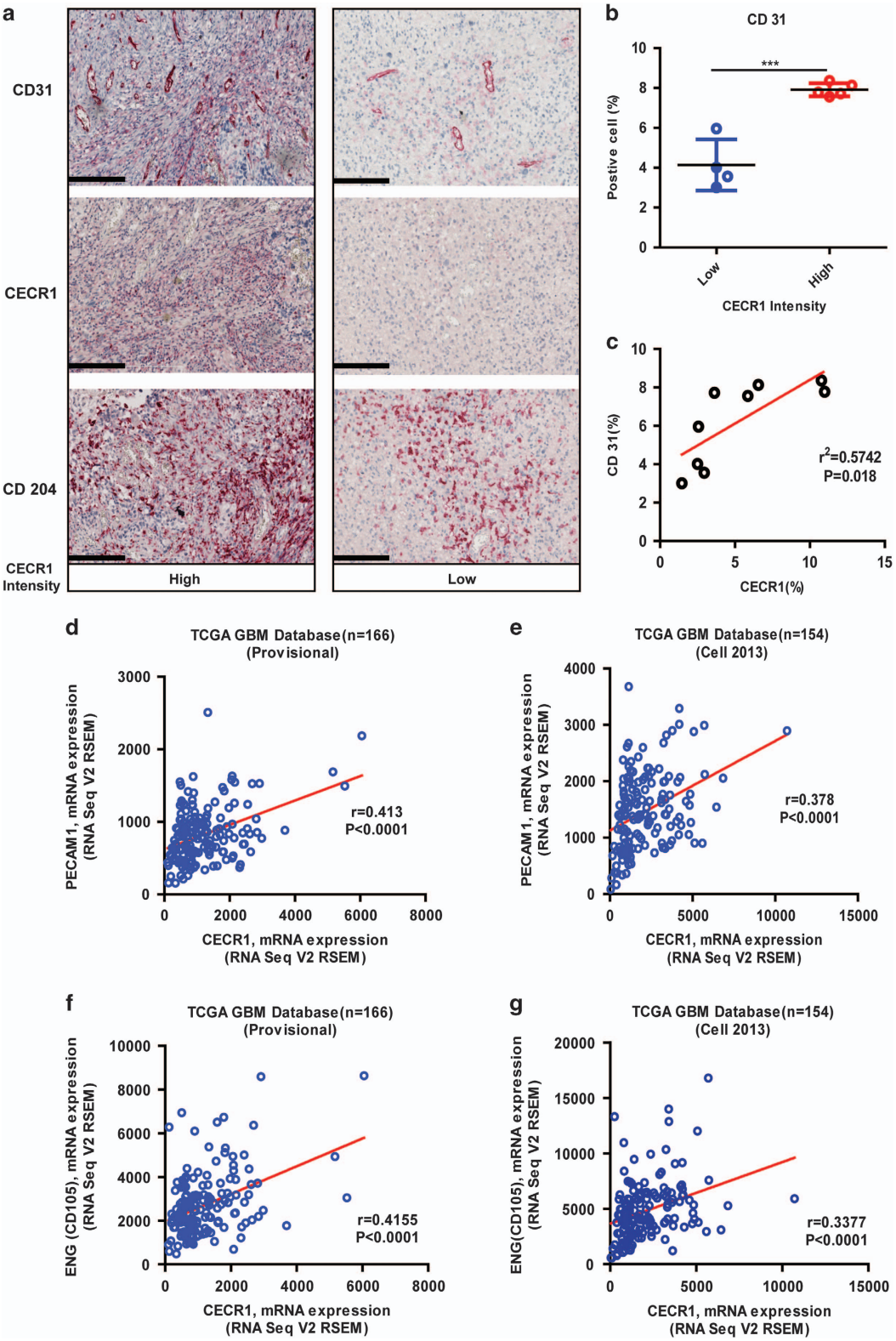

Figure 1. CECR1 levels correlates with microvascular density in human GBM. (**a**) Immunohistological staining of human GBM cross-sections for CD31, CECR1 and CD204, in samples with high CECR1 signal (column High) and low CECR1 signal (column Low; scale bar:, 200 μm). (**b**) Results of a quantitative analysis using ImageJ software of the mean percentage of CD31+ cells per image field per GBM patient in CECR1 low- and high-signal groups. (**c**) The correlation between mean %CD31+ cells and %CECR1+ cells per image field per GBM patient. (**d**) Correlation between PECAM1 and CECR1 mRNA levels in a set of 166 TCGA data set-derived GBM samples. (**e**) Correlation between PECAM1 and CECR1 mRNA levels in a second set of 154 TCGA data set-derived GBM samples. (**f**) Correlation between Endoglin and CECR1 mRNA levels in a set of 166 TCGA data set-derived GBM samples. (**g**) Correlation between Endoglin and CECR1 mRNA levels in a second set of 154 TCGA data set-derived GBM samples. ***$P < 0.01$.

contrast, expression levels of other proangiogenic genes including VEGFA were not affected (ANGPT1, ANGPT2, MMP7, MMP9, VWF, Tie-2; Supplementary Figure 5), except for IL8. The latter is more associated with the cytokine profile of M1 macrophages. Vice versa, macrophages of silenced CECR1 showed a significant decrease in expression of PDGFB (Figure 3a). These data were

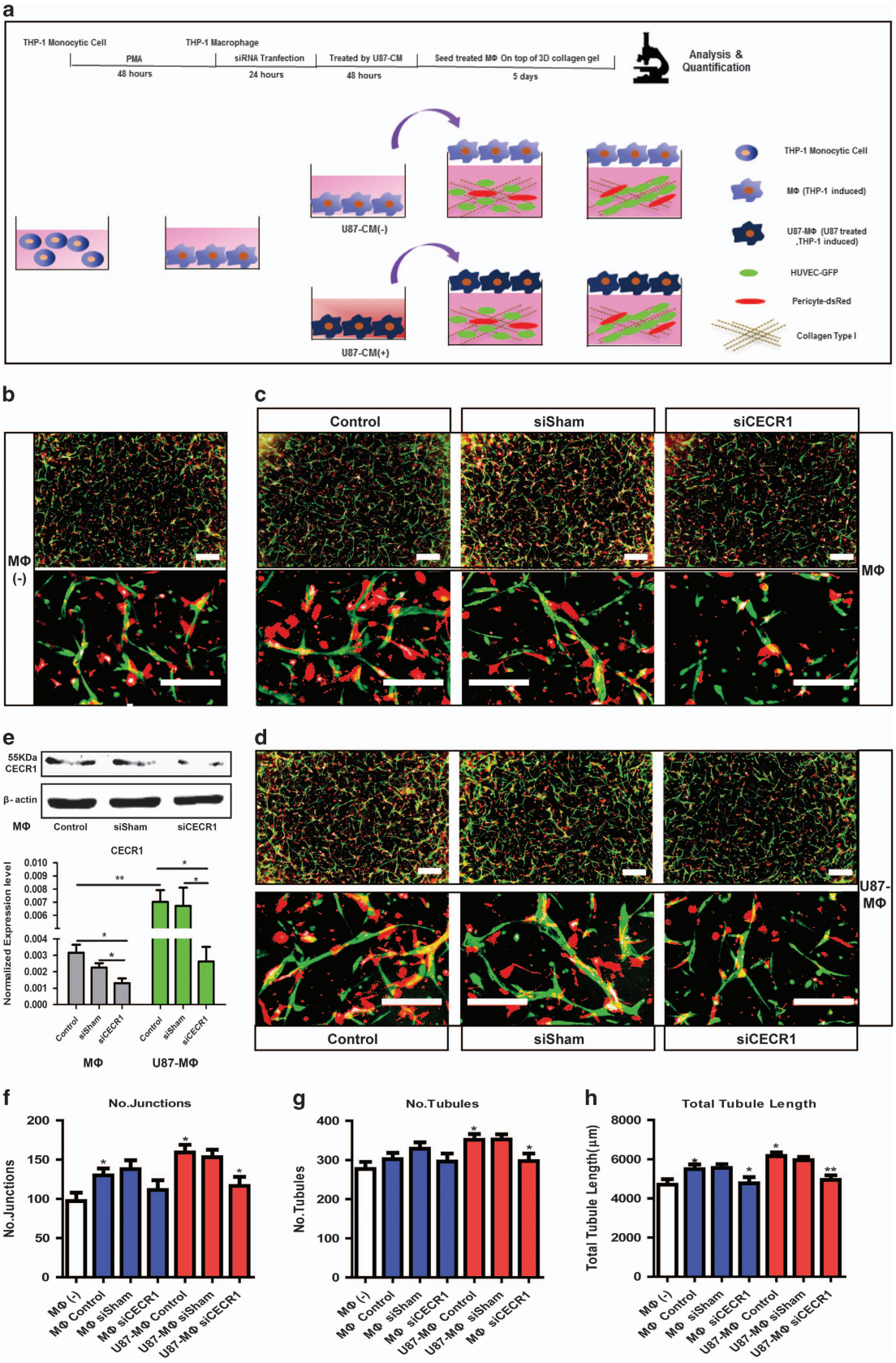

further validated by immunofluorescent staining of cytospin THP1 macrophages, showing a reduction in PDGFB signal that coincided with a reduction in CD163 (M2) marker signal in the CECR1-silenced versus control macrophages and sisham-treated macrophages (Figure 3c). This effect was CECR1 knockdown specific, as knockdown of PDGFB in THP1 macrophages did not reduce the CD163 M2 marker signal, while the PDGFB signal was clearly decreased (Figure 3c). In contrast, treatment of macrophages with rhCECR1 increased both CD163 and PDGFB mean intensity signals (Figure 3e). Quantification of the mean intensity levels of PDGFB of the different groups confirmed that PDGFB was decreased and increased by CECR1 silencing, and rhCECR1 stimulation, respectively (Figure 3d). Stimulation of THP1 macrophages with U87-derived supernatant promoted upregulation of PDGFB signal in cytospin samples. This effect was significantly reduced in siCECR1- versus sisham-treated THP1 macrophages (Figures 3f and g). A correlation between CECR1 and PDGFB levels was also found by analysis of TCGA data sets, which showed a positive correlation between PDGFB and CECR1 expression levels in a provisional set of 166 GBM samples, and was subsequently validated in a second set of 154 GBM samples (Figures 3h and i). Similar to CECR1, immunostaining of GBM samples revealed that PDGFB+ cells were mainly GAMs that express pan macrophage and M2 markers such as CD68 and CD163 (Figure 3j).

CECR1-mediated paracrine activation of macrophages promotes pericyte recruitment via PDGFB/PDGFRβ signaling in GBM

To assess the role of PDGFB in CECR1 regulation of macrophages in angiogenesis, we conducted co-culture experiments with macrophages silenced for PDGFB. Co-cultures with PDGFB-silenced macrophages seeded on top mimicked the phenotype of co-cultures that were treated by CECR1-silenced macrophages, demonstrating a general decrease of all parameters of active angiogenesis (Figures 4a–e). Co-culture analysis of siPDGFB macrophages that differentiated with exposure to U87 supernatant showed a similar negative effect on angiogenic parameters (Supplementary Figures 6a and b). This reduction was partially rescued by treating siPDGFB macrophages with rhCECR1 (siPDGFB versus siPDGFB+rhCECR1, total tubule length), indicating that the paracrine proangiogenic effect of CECR1 in macrophages is partially mediated via PDGFB (Figures 4a–e). PDGFB mediates its activity via PDGFB receptor (PDGFRβ) signaling. In GBM samples, immunostaining revealed that PDGFRβ+ cells are mainly perivascular mural cells that are closely located near CD163+ M2 macrophages (Figures 5a and b). QPCR analysis of different *in vitro* human cell types that have equivalents in GBM *in vivo*, including HUVECs, pericytes, U87, U251 and THP1 macrophages, demonstrated that PDGFRβ was mainly expressed by pericytes (Figure 5c). Confocal imaging combined with double immunostaining further confirms mural cell expression of PDGFRβ and the close localization of CD163+ GAMs in human GBMs (Figure 5d). The PDGFB/PDGFRβ ligand/receptor signaling mechanism is well known to promote mural cell proliferation and is critical for mural cell recruitment to newly formed vessels to ensure vascular coverage and stabilization. Next, we investigated the CECR1-mediated effects of THP1 macrophages on pericyte recruitment. Pericytes were evaluated for their migratory capacity in a transwell migration assay in response to paracrine factors that are present in macrophage-derived supernatants of the different groups (Figure 5e). Pericyte migration increased on stimulation by supernatant of THP1 macrophages (Figures 5f and g). Pericyte migration significantly decreased in response to supernatant derived from CECR1-silenced THP1 macrophages (Figures 5e–g). This effect was mimicked by exposure to supernatant derived from PDGFB-silenced THP1 macrophages (Figures 5f and g). To investigate whether direct binding of CECR1 to PDGFRβ in pericytes may also regulate pericyte response, co-immunoprecipitation (Co-IP) was conducted. Pull-down of PDGFRβ protein using anti-PDGFRβ-coated beads in lysates of CECR1-treated and non-treated pericytes was successfully validated. Likewise, pull-down of CECR1 using anti-CECR1-coated beads was also successful. However, it failed to demonstrate CECR1 binding to PDGFRβ protein in both conditions, indicating that there is no direct contact of CECR1 with PDGFRβ in pericytes (Supplementary Figure 7).

CECR1 activation in THP1 macrophages promotes paracrine activation of periostin and VEGFA protein production in pericytes

Further confocal immunohistochemical analysis of human GBM samples revealed co-localization of PDGFB+ perivascular mural cells with the extracellular matrix component periostin (Figure 6a). Previously, we have detected enrichment of periostin in the microvasculature of GBMs using a proteomics screen.[28] Work by others revealed an important role for periostin in recruitment of M2-like tumor-associated macrophages and subsequent support of malignant growth.[13] In line with these reports, periostin deposition was detected in close proximity of CD163+ M2 GAMs (Figure 6b). A significant positive correlation was also identified between CD163 and periostin expression in a set of 154 samples using the TCGA GBM database (Figure 6c). Similar to PDGFRβ, qPCR analysis of different *in vitro* human cell types that can be found in GBM, including HUVECs, pericytes, U87, U251 and macrophages, demonstrated that periostin was mainly expressed by pericytes (Figure 6d). Paracrine stimulation of pericytes by THP1 macrophages enhanced periostin protein levels in the co-culture setup (Figures 6e and f). THP1 macrophages stimulated with U87 supernatant during maturation further enhanced periostin protein levels (Figures 6e and f), indicating that GAMs can significantly promote periostin protein production in pericytes.

Periostin expression correlates ($r = 0.3015$; $P < 0.0001$) with CECR1 expression levels in a set of 205 samples derived from the TCGA GBM database (Figure 6g). The periostin protein levels of pericytes exposed to the paracrine activity of THP1 macrophages dropped significantly following silencing the macrophages for

Figure 2. CECR1 promotes the proangiogenic paracrine action of M2 macrophages. (**a**) Diagram showing the experimental setup of testing paracrine angiogenic activation of vascular cells in 3D co-cultures by THP1 macrophages. (**b**) Low and high-magnification fluorescent images of neo-vessel formation by HUVECs (GFP-marked) and human-derived pericytes (dsRed-marked) without THP1 macrophage stimulation. (**c**) Low- and high-magnification fluorescent images of neo-vessel formation by HUVECs (GFP-marked) and human-derived pericytes (dsRed-marked) with stimulation of non-treated (control), and sisham- or siCECR1-treated THP1 macrophages. (**d**) Low- and high-magnification fluorescent images of neo-vessel formation by HUVECs (GFP-marked) and human-derived pericytes (dsRed-marked) with stimulation of non-treated (control), and sisham- or siCECR1-treated THP1 macrophages with U87 stimulation (scale bar, 100 μm for **b**–**d**). (**e**) Upper image: western blot of CECR1 protein and β-actin loading control in THP1 macrophages. Blot represents results from three observations. Lower graph: QPCR results of CECR1 mRNA levels normalized to housekeeping genes in non-treated (control), and sisham- or siCECR1-treated THP1 macrophages, without and with U87 stimulation. $^{*}P < 0.05$; $^{**}P < 0.01$. (**f**–**h**) Quantified results of the co-culture experiment. Number of junctions, tubules and total tubule length data are shown. $^{*}P < 0.05$; $^{**}P < 0.01$. (MΦ (-) versus MΦ-control, U87 MΦ-control versus MΦ-control, MΦ-sisham versus MΦ-siCECR1, U87 MΦ-sisham versus U87 MΦ-siCECR1). Representative graphs were taken from at least three experiments. Six wells were analyzed in each experiment.

CECR1 (Figures 6h and i). Silencing of PDGFB in the THP1 macrophages also resulted in decreased periostin production by pericytes (Figures 6h and i). In support of these findings, THP1 macrophages that were treated with rhCECR1 during maturation, increased periostin protein levels produced by pericytes (Figure 6j). Similarly, periostin production by pericytes that were directly stimulated with physiological levels of PDGFB was significantly increased (Figures 6k and l). Applying the same experimental settings, CECR1 was found to regulate VEGFA production in pericytes in a macrophage-dependent manner (pericytes in response to CECR1 modulated macrophages) and macrophage-independent manner (direct CECR1 and PDGFB

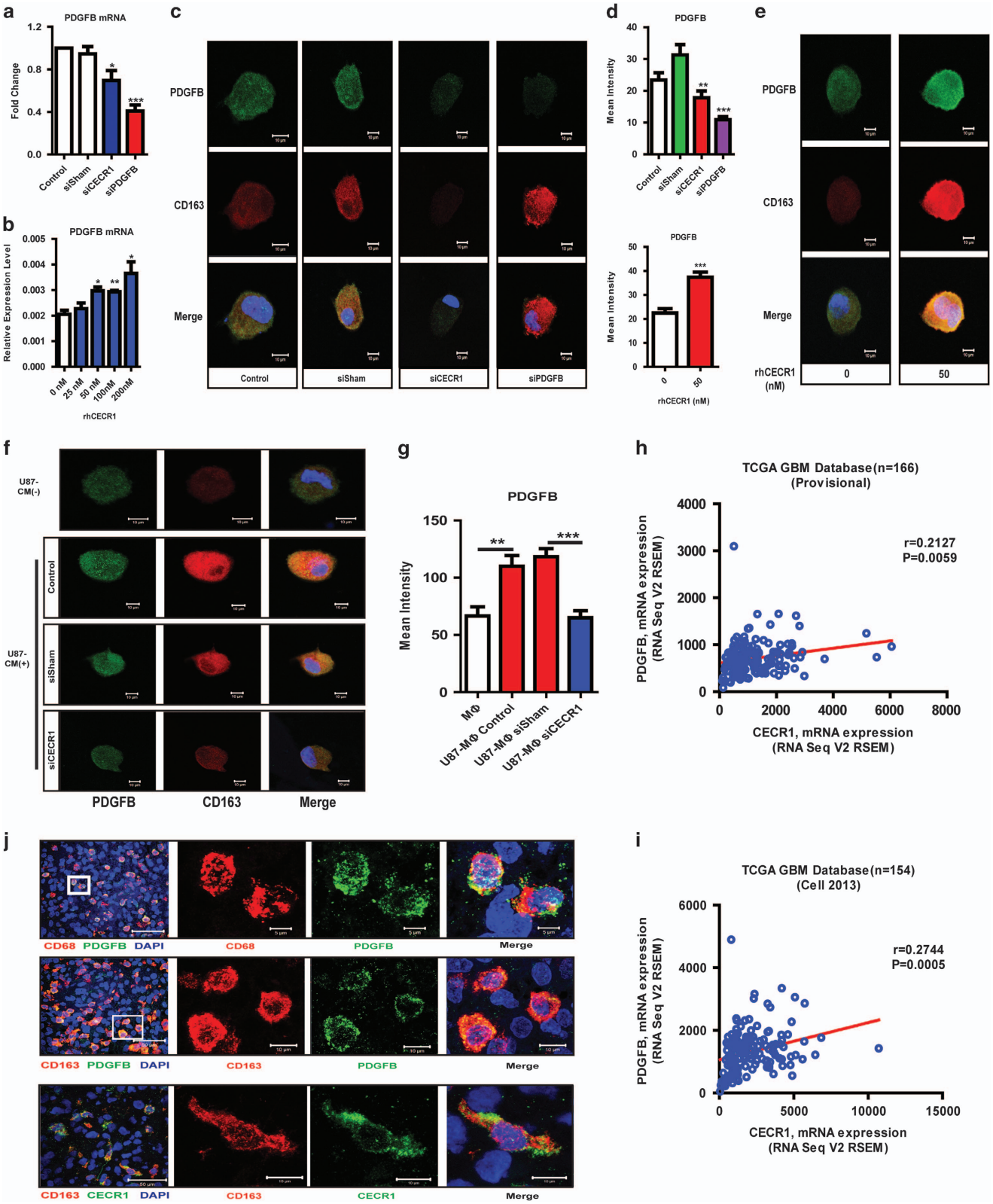

stimulation of pericytes; Supplementary Figures 8 a–d). Direct stimulation of pericytes with rhCECR1 did not enhance periostin production, but it did enhance VEGFA production (Figure 6m, Supplementary Figure 8c), indicating that the CECR1-mediated macrophage activation of periostin expression in pericytes is indirect and requires an intermediate paracrine factor, such as

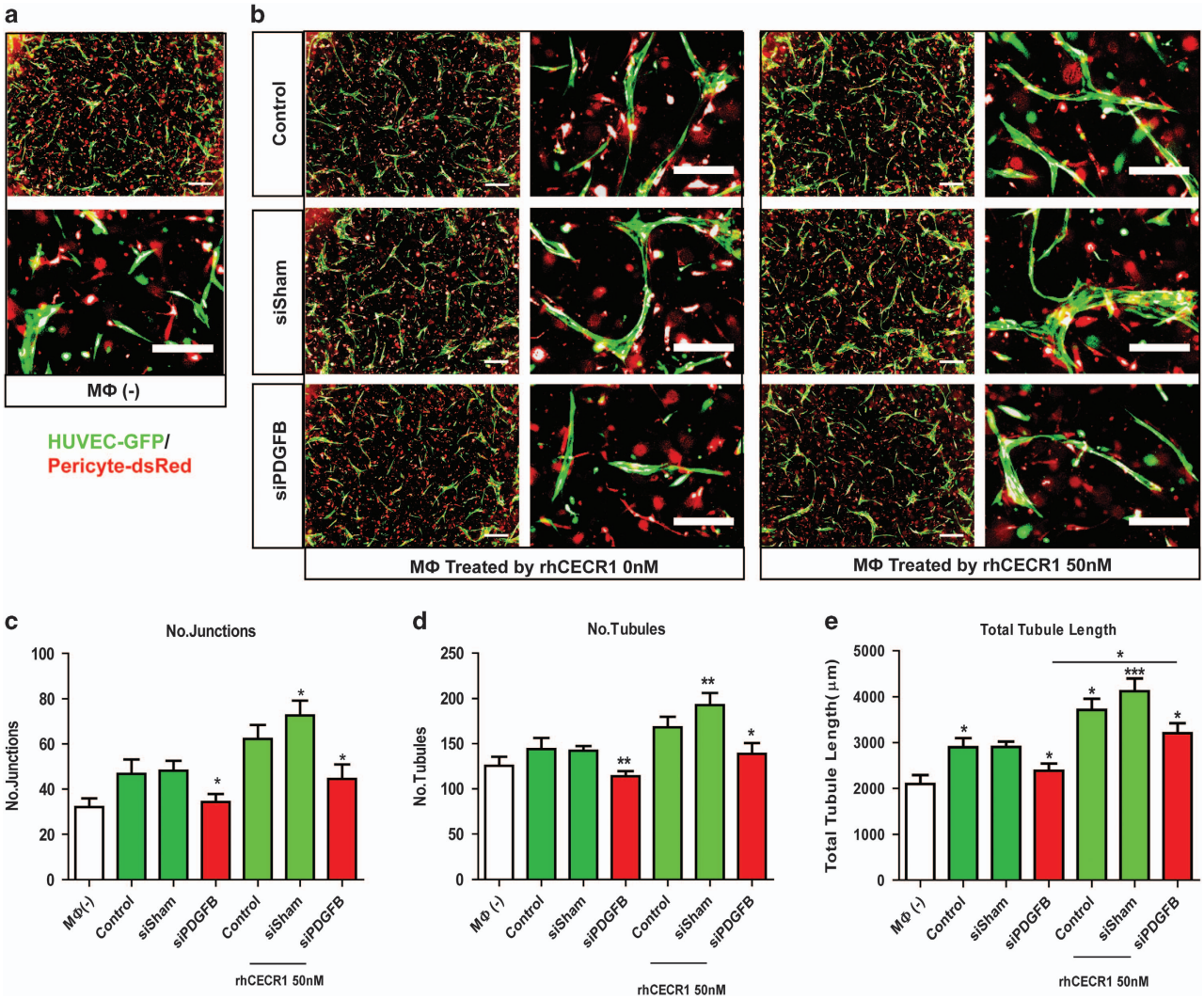

Figure 4. CECR1-mediated macrophage paracrine activation of angiogenesis is partially regulated via PDGFB. (**a** and **b**) Low- and high-magnification fluorescent images of neo-vessel formation by HUVECs (GFP-marked) and human-derived pericytes (dsRed-marked) without THP1 macrophage stimulation, and with stimulation of non-treated (control), and sisham- or siPDGFB-treated THP1 macrophages, without or with rhCECR1 rescue. (**c**–**e**) Quantified results of the co-culture experiment. Number of junctions, tubules and total tubule length data are shown. $^{*}P < 0.05$ (MΦ (-) versus MΦ-control, MΦ-sisham versus MΦ-siPDGFB, MΦ-sisham CECR1 0 nM versus 50 nM, MΦ-siPDGFB CECR1 0 nM versus CECR1 50 nM); $^{**}P < 0.01$ (MΦ-sisham CECR1 0 nM versus 50 nM in number of tubules), $^{***}P < 0.005$ (MΦ-sisham CECR1 0 nM versus 50 nM in total tubule length). Scale bar, 100 μm. $N > 10$ co-cultures in total.

Figure 3. PDGFB expression correlates with M2 GAMs and is enhanced by CECR1. (**a**) QPCR analysis of PDGFB mRNA levels normalized to housekeeping genes in non-treated (control), and sisham- or siCECR1- or siPDGFB-treated THP1 macrophages. $^{*}P < 0.05$; $^{***}P < 0.005$ versus control and sham conditions. Experiments were repeated at least three times. (**b**) QPCR analysis of PDGFB mRNA levels normalized to housekeeping genes in THP1 macrophages treated with different concentrations of rhCECR1 from three experiments. $^{*}P < 0.05$; $^{***}P < 0.005$ versus no rhCECR1 stimulation. (**c**) Image panel shows immunofluorescent staining of PDGFB and CD163, and merged images of cytospin non-treated (control), and sisham- or siCECR1- or siPDGFB-treated THP1 macrophages (scale bar, 10 μm). (**d**) Graph shows mean PDGFB intensity of each treatment group. $^{**}P < 0.01$; $^{***}P < 0.005$ versus sisham condition. Experiments were repeated at least three times. (**e**) Image panel shows immunofluorescent staining of PDGFB and CD163, and merged images of cytospun non-treated (control), and rhCECR1-treated THP1 macrophages (scale bar, 10 μm). Graph at the right shows mean PDGFB intensity of rhCECR1 stimulation versus no stimulation. $^{***}P < 0.005$ versus no treatment condition. (**f**) Immunofluorescent staining of PDGFB (green) and CD163 (red), and merged images of cytospin non-treated controls with exposure to U87 supernatant U87 conditioned medium (CM), and THP1 macrophages treated with sisham +U87 supernatant or siCECR1+U87 supernatant. (**g**) Mean PDGFB intensity of each treatment group from at least three experiments. $^{**}P < 0.01$; $^{***}P < 0.005$. (**h**) Correlation between PDGFB and CECR1 mRNA levels in a set of 166 TCGA data set-derived GBM samples. (**i**) Correlation between PDGFB and CECR1 mRNA levels in a second set of 154 TCGA data set-derived GBM samples. (**j**) Low- and high-magnification confocal images of double immunofluorescent staining of CD68, CD163 and PDGFB, CECR1 in human GBM sections (scale bars, 50 μm (left panel); 5 μm (right upper panel), 10 μm (right lower panel)).

PDGFB. In line with these findings, direct stimulation of pericytes with PDGFB promoted pericyte migration, and silencing of periostin in pericytes (Figure 6n) inhibited this response (Figures 6o and p).

Further evidence for the involvement of periostin in angiogenesis and cell migration is provided by correlation analysis of periostin expression in three different TCGA-derived human GBM data sets (Supplementary Figure 9a). Overlap analysis identified a

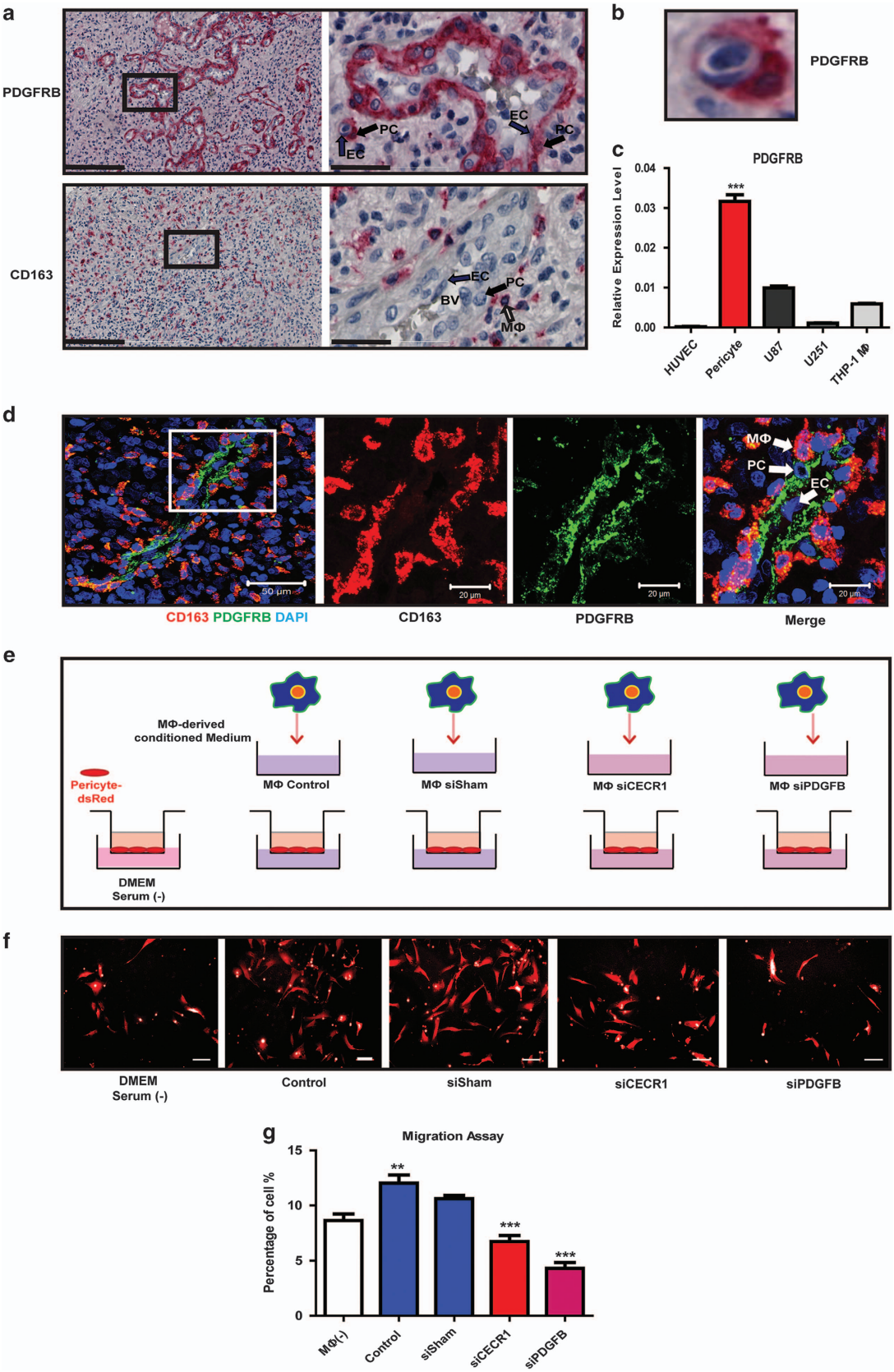

set of 139 genes that was significantly correlated with periostin expression in the three GBM gene sets (Supplementary Figure 9b). Functional annotation of the 139 genes identified the top 20 of the significant biological processes including angiogenesis-related GO terms such as 'blood vessel morphology', 'angiogenesis', 'blood vessel development' and 'cardiovascular system development' (Supplementary Figure 9c). GO terms associated with cell migration such as 'cell adhesion', and 'extracellular matrix disassembly' were also identified (Supplementary Figure 9c). Taken together, the data reveal a link between periostin expression by pericytes and CECR1-mediated macrophage paracrine activity.

DISCUSSION

The main findings of this study are: (i) expression of CECR1 is positively correlated with microvascular density in glioblastoma; (ii) CECR1 expression by GAMs promotes angiogenesis in a 3D co-culture assay; (iii) the level of CECR1 regulates PDGFB production in GAMs; (iv) the CECR1–PDGFB-mediated cross talk between macrophages and pericytes promotes migration of pericytes and contributes to new vessel formation; (v) macrophage–pericyte CECR1–PDGFB–PDGFRβ signaling upregulates the expression of the proangiogenic extracellular matrix component periostin in pericytes.

Current knowledge of the proangiogenic capacities of GAMs mainly concerns the effects of these cells on vascular endothelial cells.[29] The regulation of perivascular cells, such as pericytes, by GAMs, is rarely studied. In this study, we describe the proangiogenic role of CECR1 that is mediated via an autocrine feedback loop in which CECR1 production in M2-like GAMs enhances PDGFB expression and secretion. Furthermore, CECR1 from M2-like GAMs enhances VEGFA production in pericytes. PDGFB/PDGFRβ signaling is crucial for the vascular maturation process in angiogenesis, during which newly formed microvessels secrete PDGFB to guide perivasular coverage by pericytes as well as VEGFA production. PDGFB secreted by M2-like GAMs promotes both pericyte migration and angiogenesis, as shown by our migration and 3D co-culture data, respectively. Depletion of PDGFB mimicked the vascular phenotype that was triggered by depletion of its putative upstream molecule, CECR1.

Periostin is an extracellular matrix protein that is specifically present in the basal membrane of the microvasculature of GBMs.[19] In the present study, we identified periostin as a potent downstream target of the macrophage CECR1–PDGFB paracrine signaling cascade (see Supplementary Data Figure 10). Pericytes are defined by their singular perivascular position, their remarkable dendrite-like morphology and their expression of PDGFRβ and NG-2.[30] Pericytes are multifunctional cells,[31] being vital cells for vessel construction, maintenance and the regulation of the vascular physiology.[32] Pericyte dysfunction could lead to delay in blood vessel maturation, and contributes to vascular instability and leakage.[33] Pericytes also contribute to recruitment of immune cells, including monocytes, during inflammation.[34] A process of mutual activation between GAMs and pericytes during tumor angiogenesis has been previously identified. In tumors, the paracrine influence of GAMs leads to activation of the PDGFB–SOX17 axis, which is initiated by tumor cells and leads to pericyte production of IL-33.[35] In addition, tumor-associated macrophages secrete MMP9, which has been shown to enhance the recruitment of pericyte precursor cells into the tumor microenvironment.[36] The present data demonstrate the proangiogenic function of CECR1 in macrophages, mediated via paracrine regulation of PDGFB. The relation between CECR1, angiogenesis and vascular density is reflected by the hyper-inflammatory response in patients with a CECR1 loss of function mutation.[26] One of the most prominent symptoms displayed by these patients was early-onset stroke and profound vasculopathy. Similarly, vascular instability was observed in zebrafish with CECR1 knockdown. In previous studies, we pointed out that CECR1 in GBM is mainly expressed by M2-like GAMs. We also discovered that CECR1 acts as a potent polarizing factor in GAMs differentiation towards the M2-like phenotype. CECR1 activity also increased the pro-tumoral function of M2 macrophages in a paracrine manner.[37] In the current study, we have shown that CECR1 activity in GAMs enhances PDGFB mRNA and protein production levels. In line with these findings, PDGFB was previously reported not only to be expressed by activated endothelial cells, but also by M2-like GAMs.[38] Elevated levels of PDGFB produced in malignant cancers upregulate erythropoietin expression in stromal cells via activation of PDGRB that accelerates tumor angiogenesis.[39] The CECR1–PDGFB–PDGFRβ axis that is revealed in this study points to a putative CECR1-mediated functional cross talk between macrophages and pericytes, guiding the process of vascular maturation and development. This process may be involved in the vascular symptoms observed in patients with CECR1 mutations.[25] However, it has to be acknowledged that the qPCR screen only included a limited selection of cytokines that were known to affect angiogenesis and were reportedly produced by macrophages. Future studies should aim on expanding the current screen data using a genome-wide approach to identify additional (secreted) factors that may be regulated by CECR1 in GAMs.

Aberrant vessel morphology with abnormal pericyte coverage is considered as one of the classical hallmarks of tumor vasculature in malignant tumors including GBM. Recent studies of pericytes have revealed hyperplasia of this cell type in GBM.[40] The function of pericytes in malignant tumors is not only restricted to support vascular growth, but as a potent producer of VEGFA, perivascular pericytes also protect the tumor microvasculature against disintegration during anti-VEGFA therapy by elevating local VEGFA levels.[31] Furthermore, pericytes in glioma were shown to produce other angiogenic molecules like HGF, TGFβ1 and prostaglandins. Pericytes also inhibit the activation of T cells and thereby induce immunosuppression in glioma,[41] while expressing plasminogen urokinase in support of the self-renewal and invasion of glioma initiating cells.[42] Based on these reports, we can conclude that

Figure 5. CECR1-mediated paracrine activation of macrophages may promote pericyte recruitment via PDGFB/PDGFRβ signaling in GBM. (**a**) Low (right panel) and high (left panel) immunohistological staining of PDGFRβ and CD163 in human GBM sections. Black arrows indicate pericytes and endothelial cells (EC) forming blood vessels (BV). White arrow indicates macrophages (Mφ) (Scale bar, 200 μm (left panel); 40 μm (right panel)). (**b**) High-magnification image of PDGFRβ immunohistological staining in human GBM sections. (**c**) QPCR analysis of PDGFRβ mRNA expression levels normalized to housekeeping genes in HUVECs, pericytes, U87, U251 and THP1 macrophages from three experiments. $^{***}P < 0.001$ (pericytes versus other cell types). (**d**) Confocal images of CD163 and PDGFRβ double immunofluorescent staining in human GBM sections. White arrows indicate pericytes, endothelial cells (EC) and macrophages (Mφ). Scale bars, 50 μm (left panel); 20 μm (right panel). (**e**) Diagram of the experimental setup of the transwell migration assay of pericytes (dsRed-marked) seeded on top of the transwell. Cell migration was towards a lower chamber with DMEM medium only, or with supernatant derived from non-treated (control) macrophages, and sisham- or siCECR1-treated macrophages. (**f**) Panel of fluorescent images of dsRed-marked pericytes that have migrated through the transwell setting in response to the different conditions (DMEM only, or in response to supernatant of non-treated macrophages (control), or sisham-, siCECR1- or siPDGFRβ-treated macrophages). (**g**) Quantified results of the transwell migration assay. $^{**}P < 0.01$ (MΦ(-) versus Control); $^{***}P < 0.005$ (sisham versus siCECR1; sisham versus siPDGFB), $N > 6$ migration assays per condition.

pericytes have multiple significant roles in promoting angiogenesis and tumor progression in glial tumors.

In this study, we have identified periostin as a downstream target of PDGFB signaling in pericytes. Periostin was identified as a proangiogenic extracellular matrix component in glioma.[28] As a multifunctional protein, it is involved in various carcinogenic processes such as the regulation of cell migration and the epithelial–mesenchymal transition in cancer cells, mainly via activation of cell focal adhesion kinases through cell binding to integrins.[43] Recently, periostin was shown to have a role in the

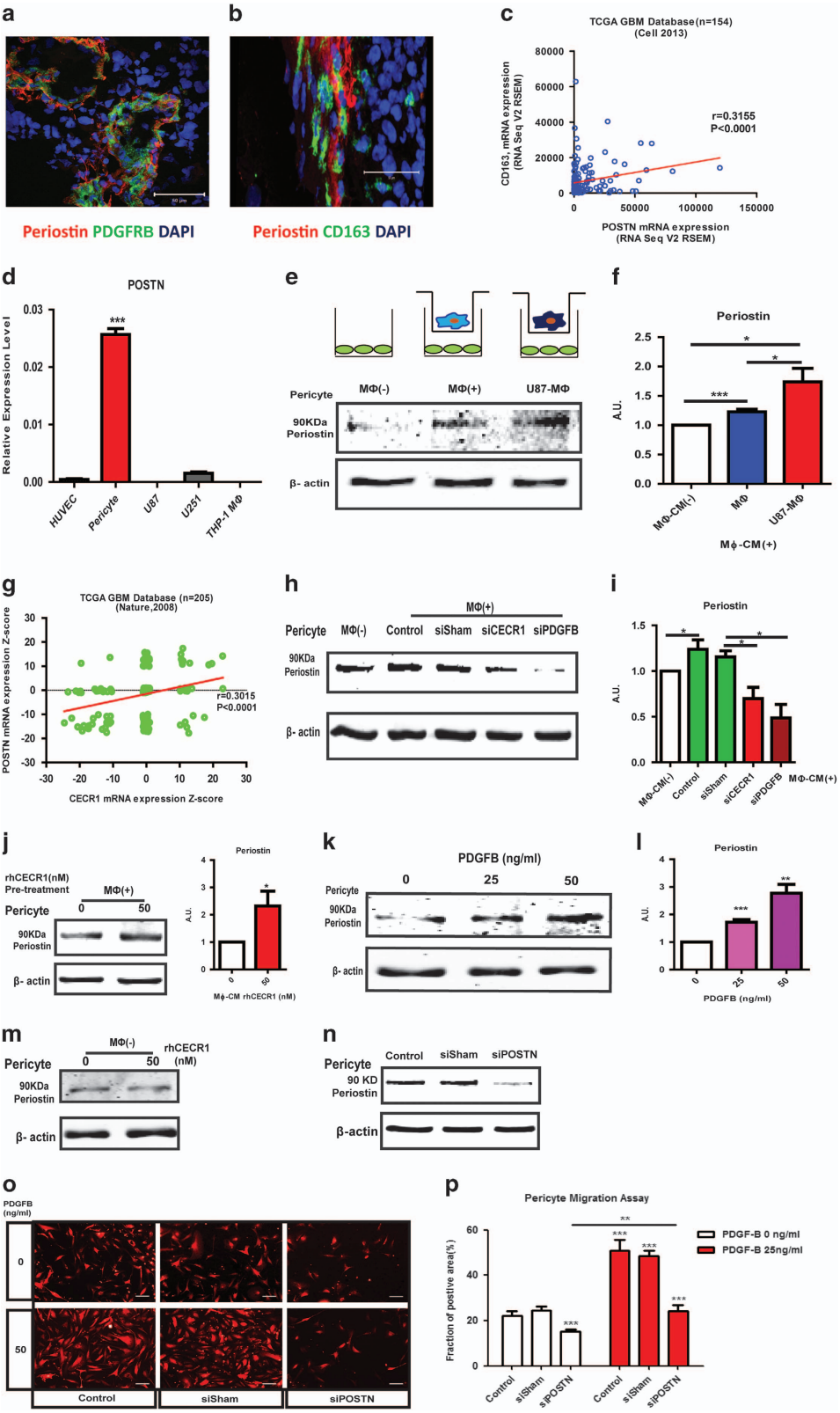

recruitment of M2-like GAMs in GBM[13] and to mediate the resistance to anti-VEGFA therapy by increasing expression of caveolin-1, HIF-1α and VEGFA.[44] In addition, periostin is expressed by mammary stromal cells in breast cancer where it is involved in actively maintaining a breast cancer stem cell niche via the canonical WNT signaling pathway.[45] In pancreatic carcinoma, the expression of periostin was found upregulated in response to PDGFB stimulation.[46] Our data provide evidence that the modulation of CECR1 in macrophages influences the expression of periostin in pericytes via PDGFB-mediated paracrine signaling.

In conclusion, this study demonstrates that in glioblastoma CECR1 produced by M2-like GAMs regulates the cross talk between macrophages and pericytes via paracrine PDGFB–PDGFRβ signaling, promoting pericyte recruitment and migration, and tumor angiogenesis. The proangiogenic function of the CECR1–PDGFB–PDGFRβ signaling cascade is related to the expression of periostin by pericytes. This new knowledge on complex interaction between the immuno apparatus and vascular cells in the process of tumor neo-angiogenesis could lead to better immune-modulatory and anti-angiogenic strategies for the treatment of GBM in the future.

MATERIALS AND METHODS

Patient samples

Patient samples of glioblastoma were collected from the Department of Pathology, Erasmus Medical Center with the approval of committee of research ethics and all the subjects. All the samples were diagnosed as glioblastoma by a board certificated pathologist (JMK).

Cell culture

Human monocytic cell line THP1 (authenticated and tested mycoplasma free), obtained from the Department of Hematology, Erasmus Medical Center, was maintained in culture in RPMI-1640 (Lonza, Breda, The Netherlands) supplemented with 10% fetal bovine serum and 1% penicillin/streptomycin. THP1 cells were differentiated into macrophage-like cells by PMA (Sigma, Stockholm, Sweden) at a concentration of 100 ng/ml for 48 h. Recombinant human CECR1 protein (rhCECR1) was added to the macrophage cultures at a concentration gradient of 0, 12.5, 25, 50, 100, 200 nM for 96 h.

HUVECs (Lonza) and HUVECs transfected with a lentiviral vector encoding GFP were cultured in EGM-2 endothelial medium (Lonza) with 1% penicillin/streptomycin.

Human brain vascular pericytes with and without lentiviral transfection of a vector encoding for dsRed, and GBM cell lines U87 and U251, purchased from ATCC, were maintained in DMEM (Lonza) with 10% fetal bovine serum and 1% penicillin/streptomycin. Pericytes were treated with recombinant human PDGFB (Sigma) at different concentrations according to the specifications of the different assays. All cultured cells were checked to be negative for mycoplasma contamination. HUVECs and pericytes were authenticated by supplier and were tested mycoplasma free.

siRNA transfection

siCECR1 (5′-GUGCCAAAGGCUUGUCCUA-3′, 5′-CUUCCACGCCGGAGAAACA-3′, 5′-GCCCAAAGCUAGUUAGUAC-3′, 5′-UCGCAGAAUCCAUCCGAAU-3′); siPDGFB (5′-CCGAGGAGCUUUAUGAGAU-3′, 5′-GAAGAAGGAGCCUGGGUUC-3′, 5′-GCAAGCACCGGAAAUUCAA-3′, 5′-GGGCCGAGUUGGACCUGAA-3′), siPOSTN (5′-CCGAAGCUCUUAUGAAGUA-3′) and scrambled siRNA (5′-UGGUUUACAUGUCGACUAA-3′, 5′-UGGUUUACAUGUUGUGUGA-3′, 5′-UGGUUUACAUGUUUUCUGA-3′, 5′-UGGUUUACAUGUUUUCCUA-3′) (siSham) were purchased from Dharmacon (GE Health Care, Lafayette, LA, USA). Macrophages were transfected with SiCECR1 and siPDGFB using transfection buffer 2 (Dharmacon, GE Health Care); pericytes or pericytes-dsRed were transfected with siPOSTN using transfection buffer 1 (Dharmacon, GE Health Care) according to manufacturer's instructions (see Supplementary Materials and Methods for details).

RNA isolation and RT-qPCR

Total RNA was isolated from macrophages and pericytes using RNA isolation kit (Bioline, London, UK) and cDNA was synthesized by sensi-fast cDNA synthesis kit (Bioline). Transcripts of CECR1, PDGFB and POSTN were measured and normalized to β-actin in macrophages and pericytes (for primers sequences, see Supplementary Table 1).

Transwell co-culture

Macrophages were seeded in 0.4 μm transwell insert (Fisher Scientific, Denver, CO, USA) and were treated with U87-derived conditioned medium or recombinant human (rh)CECR1 protein for 48 h followed by co-culture with pericytes for extra 72 h. The pericytes were collected afterwards for performing downstream assays.

Co-immunoprecipitation

Pericytes cultured in serum-free DMEM medium were treated with/without 100 nM CECR1 for 6 h. The cells were collected in NP40 lysis buffer followed by incubation on ice for 30 min and were centrifuged for 12 min at 13 000 r.p.m. The supernatant was collected for co-immunoprecipitation. The 1.5 mg Dynabeads (Life Technologies, Bleiswijk, The Netherlands) were incubated with anti-PDGFRβ (CST, Leiden, The Netherlands) antibody or Isotype control from the same host (CST) for 10 min at room temperature followed by gently washing using the provided washing buffer and magnet separation (Life Technologies). A total 100 μg of lysate was added to the Dynabeads–antibody complex and incubated for 48 h at 4 °C. The formed Dynabeads–antibody–antigen complex was washed followed by elution of the target antigen at 70 °C for 10 min in provided elution buffer

Figure 6. CECR1 activation in THP1 macrophages promotes paracrine activation of periostin protein production in pericytes. (**a** and **b**) Confocal images of imunohistological stainings of periostin, PDGFRβ and CD163 in human GBM sections. Scale bar, 50 μm. (**c**) Correlation between CD163 and periostin mRNA levels in a set of 154 TCGA data set-derived GBM samples. (**d**) QPCR analysis of periostin mRNA expression levels normalized to housekeeping genes in HUVECs, pericytes, U87, U251 and THP1 macrophages from three experiments. $^{***}P < 0.001$ (pericytes versus other cell types). (**e**) Diagram showing experimental setup with pericytes (green) co-cultured with macrophages without (light blue) and with U87 pre-stimulation (dark blue) seeded in filter insert. Western blot shows periostin and β-actin protein levels in pericytes of the different treatment groups. (**f**) Quantitative results of western blot analysis normalized to β-actin loading control from four experiments. $^{*}P < 0.05$; $^{***}P < 0.005$. (**g**) Correlation between periostin and CECR1 mRNA levels in a set of 205 TCGA data set-derived GBM samples. (**h**) Western blot shows periostin and β-actin protein levels in pericytes treated with no macrophages, with non-transfected macrophages (control), and macrophages transfected with sisham, siCECR1 or siPDGFRβ. (**i**) Quantitative results of western blot analysis normalized to β-actin loading control from four experiments. $^{*}P < 0.05$. (**j**) Western blot shows periostin and β-actin protein levels in pericytes treated with macrophages with and without pre-treatment with rhCECR1. Graph shows quantitative results of western blot analysis normalized to β-actin loading control of at least four experiments. $^{*}P < 0.05$ versus no rhCECR1 stimulation. (**k**) Western blot shows periostin and β-actin protein levels in pericytes treated with different concentrations of PDGFB. (**l**) Quantitative results of western blot analysis normalized to β-actin loading control from at least three experiments. $^{**}P < 0.01$; $^{***}P < 0.005$ versus no PDGFB stimulation. (**m**) Representative western blot of three independent experiments, showing periostin and β-actin protein levels in pericytes treated with rhCECR1. (**n**) Western blot of periostin protein and β-actin loading control in pericytes with siPOSTN treatment, sisham or no treatment blot represents results from three observations. (**o**) Panel of fluorescent images of dsRed-marked pericytes that have migrated through the transwell setting in response to the different conditions (in response to supernatant of non-treated macrophages (control), or sisham- or siperiostin-treated macrophages), with and without PDGFB stimulation (scale bar, 50 μm). (**p**) Quantified results of the transwell migration assay from three experiments. $^{**}P < 0.01$ (siPOSTN versus PDGFB+siPOSTN); $^{***}P < 0.005$ (sisham versus siPOSTN; control versus PDGFB +control; sisham versus PDGFB+sisham).

with SDS loading buffer, followed by SDS–PAGE and western blotting. Whole lysates and the supernatants of the Dynabeads–antibody–antigen complex of every condition were loaded on the gel as internal controls.

Western blot

A total 20 μg of total protein lysate derived from macrophages and pericytes was loaded onto 10% SDS–PAGE gel and blotted to Nitro cellulous membranes followed by blocking and incubation of primary antibody. Protein levels were assessed by immunoblotting using specific antibodies against CECR1 (Sigma, 1:200), Periostin (R&D, Minneapolis, MN, USA, 1:200), PDGFRβ (Abcam, Milton, UK, 1:10000), and β-actin (Abcam, 1:500) as a loading control, followed by incubation with secondary antibodies (IRdye 680 CW, IRDye 800 CW, Licor Bioscience, Lincoln, NE, USA) and detection of signals using the Odyssey imaging system (Licor Bioscience).

Immunostaining

Four micrometers of adjacent sections were used for immunohistochemical and immunofluorescence analysis. Immunostaining and slide scanning were performed according to the protocol described previously.[47] Macrophages were fixed using 4% paraformaldehyde/phosphate-buffered saline, followed by antibody incubation. All fluorescence-labeled samples were analyzed under the confocal microscope LSM 700 (Zeiss, Breda, The Netherlands). Five areas in high-magnification field were randomly selected from each slide and blind quantified using ImageJ (Antibodies applied were listed in Supplementary Table 2).

Transwell migration assay

A total 7000 pericytes-dsRed with transfected with siPOSTN, siSham and non-transfected controls were seeded into the top compartment of the Fluor block 8 μm transwell inserts (Fisher Scientific). Recombinant PDGFB protein was added in the lower chamber with serum-free DMEM medium. Serum-free macrophage-conditioned medium from sisham, siCECR1, siPDGFB and non-transfected control macrophages was added into the lower chamber. After 24 h of migration, the pictures from five randomly selected areas under × 10 view were taken under a fluorescent microscope for image quantification by ImageJ.

3D collagen tubule-formation assay

HUVEC-GFP and pericyte-dsRed were co-cultured in 96-well plate at 5:1 ratio within a 3D culture environment of bovine collagen type I (Gibco, Gaithersburg, MD, USA) supplemented with SCF-1, SDF-1α and IL-3, as described previously.[48] Three hundred macrophages with different conditions were seeded on top of the collagen gel and maintained for 5 days. At the fifth day, tubule formation was captured by fluorescent microscope and blind quantified by Angiosys 1.0.

TCGA database

Three GBM data sets were obtained from TCGA via the c-Bioportal provided by the Memorial Sloan Kettering Cancer Center. Genes that positively correlated with POSTN expression (cutoff point: spearman $r > 0.4$) in all three GBM database were selected for pathway analysis by String.

Statistics

Data from clinical samples were analyzed by Mann–Whitney *U*-test and Spearman Correlation using SPSS 21.0 (IBM, Chicago, IL, USA). All *in vitro* data were tested using unpaired two-tailed Student's *T*-test or by one-way analysis of variance followed by Tukey's *post hoc* test where appropriate (Significance levels $P < 0.05$). All data are presented in mean ± s.e.m. unless otherwise stated.

CONFLICT OF INTEREST

The authors declare no conflict of interest.

ACKNOWLEDGEMENTS

CZ was supported by the Chinese Scholar Council (201206230102). CC was supported by the Netherlands Foundation for Cardiovascular Excellence and by The Netherlands Cardiovascular Research Initiative: an initiative with support of the Dutch Heart Foundation, (CVON2014-11 RECONNECT), VIDI grant 91714302, the Erasmus MC fellowship grant and the RM fellowship grant of the UMC Utrecht. We thank CardioGenx B.V. for providing the recombinant CECR1.

REFERENCES

1 Wen PY, Kesari S. Malignant gliomas in adults. *N Engl J Med* 2008; **359**: 492–507.
2 Das S, Marsden PA. Angiogenesis in glioblastoma. *N Engl J Med* 2013; **369**: 1561–1563.
3 Prosniak M, Harshyne LA, Andrews DW, Kenyon LC, Bedelbaeva K, Apanasovich TV *et al.* Glioma grade is associated with the accumulation and activity of cells bearing M2 monocyte markers. *Clin Cancer Res* 2013; **19**: 3776–3786.
4 Gilbert MR. Antiangiogenic therapy for glioblastoma: complex biology and complicated results. *J Clin Oncol* 2016; **34**: 1567–1569.
5 Takano S. Glioblastoma angiogenesis: VEGF resistance solutions and new strategies based on molecular mechanisms of tumor vessel formation. *Brain Tumor Pathol* 2012; **29**: 73–86.
6 Ferrara N. Pathways mediating VEGF-independent tumor angiogenesis. *Cytokine Growth Factor Rev* 2010; **21**: 21–26.
7 Hambardzumyan D, Gutmann DH, Kettenmann H. The role of microglia and macrophages in glioma maintenance and progression. *Nat Neurosci* 2016; **19**: 20–27.
8 Lu-Emerson C, Snuderl M, Kirkpatrick ND, Goveia J, Davidson C, Huang YH *et al.* Increase in tumor-associated macrophages after antiangiogenic therapy is associated with poor survival among patients with recurrent glioblastoma. *Neuro Oncol* 2013; **15**: 1079–1087.
9 Chen X, Zhang L, Zhang IY, Liang J, Wang H, Ouyang M *et al.* RAGE expression in tumor-associated macrophages promotes angiogenesis in glioma. *Cancer Res* 2014; **74**: 7285–7297.
10 Brandenburg S, Müller A, Turkowski K, Radev Y, Rot S, Schmidt C *et al.* Resident microglia rather than peripheral macrophages promote vascularization in brain tumors and are source of alternative pro-angiogenic factors. *Acta Neuropathol* 2016; **131**: 365–378.
11 Nijaguna MB, Patil V, Urbach S, Shwetha SD, Sravani K, Hegde AS *et al.* Glioblastoma-derived macrophage colony-stimulating factor (MCSF) induces microglial release of insulin-like growth factor-binding protein 1 (IGFBP1) to promote angiogenesis. *J Biol Chem* 2015; **290**: 23401–23415.
12 Li W, Graeber MB. The molecular profile of microglia under the influence of glioma. *Neuro Oncol* 2012; **14**: 958–978.
13 Squadrito ML, De Palma M. A niche role for periostin and macrophages in glioblastoma. *Nat Cell Biol* 2015; **17**: 107–109.
14 Pong WW, Walker J, Wylie T, Magrini V, Luo JQ, Emnett RJ *et al.* F11R is a novel monocyte prognostic biomarker for malignant glioma. *PLoS One* 2013; **8**: e77571.
15 Komohara Y, Ohnishi K, Kuratsu J, Takeya M. Possible involvement of the M2 anti-inflammatory macrophage phenotype in growth of human gliomas. *J Pathol* 2008; **216**: 15–24.
16 Gabrusiewicz K, Rodriguez B, Wei J, Hashimoto Y, Healy LM, Maiti SN *et al.* Glioblastoma-infiltrated innate immune cells resemble M0 macrophage phenotype. *JCI Insight* 2016; **1**: e85841.
17 Bowman RL, Klemm F, Akkari L, Pyonteck SM, Sevenich L, Quail DF *et al.* Macrophage ontogeny underlies differences in tumor-specific education in brain malignancies. *Cell Rep* 2016; **17**: 2445–2459.
18 Zhu C, Kros JM, van der Weiden M, Zheng P, Cheng C, Mustafa DA. Expression site of P2RY12 in residential microglial cells in astrocytomas correlates with M1 and M2 marker expression and tumor grade. *Acta Neuropathol Commun* 2017; **5**: 4.
19 Roma-Lavisse C, Tagzirt M, Zawadzki C, Lorenzi R, Vincentelli A, Haulon S *et al.* M1 and M2 macrophage proteolytic and angiogenic profile analysis in atherosclerotic patients reveals a distinctive profile in type 2 diabetes. *Diab Vasc Dis Res* 2015; **12**: 279–289.
20 Nakamura R, Sene A, Santeford A, Gdoura A, Kubota S, Zapata N *et al.* IL10-driven STAT3 signalling in senescent macrophages promotes pathological eye angiogenesis. *Nat Commun* 2015; **6**: 7847.
21 Jetten N, Verbruggen S, Gijbels MJ, Post MJ, De Winther MP, Donners MM. Anti-inflammatory M2, but not pro-inflammatory M1 macrophages promote angiogenesis *in vivo*. *Angiogenesis* 2014; **17**: 109–118.
22 Potente M, Gerhardt H, Carmeliet P. Basic and therapeutic aspects of angiogenesis. *Cell* **146**: 873–887.
23 Lin L, Chen YS, Yao YD, Chen JQ, Chen JN, Huang SY *et al.* CCL18 from tumor-associated macrophages promotes angiogenesis in breast cancer. *Oncotarget* 2015; **6**: 34758–34773.
24 Zhu C, Mustafa D, Zheng PP, van der Weiden M, Sacchetti A, Brandt M *et al.* Activation of CECR1 in M2-like TAMs promotes paracrine stimulation-mediated glial tumor progression. *Neuro Oncol* 2017; **19**: 648–659.

25 Navon Elkan P, Pierce SB, Segel R, Walsh T, Barash J, Padeh S *et al.* Mutant adenosine deaminase 2 in a polyarteritis nodosa vasculopathy. *N Engl J Med* 2014; **370**: 921–931.
26 Zhou Q, Yang D, Ombrello AK, Zavialov AV, Toro C, Zavialov AV *et al.* Early-onset stroke and vasculopathy associated with mutations in ADA2. *N Engl J Med* 2014; **370**: 911–920.
27 Brennan CW, Verhaak RG, McKenna A, Campos B, Noushmehr H, Salama SR *et al.* The somatic genomic landscape of glioblastoma. *Cell* 2013; **155**: 462–477.
28 Mustafa DAM, Dekker LJ, Stingl C, Kremer A, Stoop M, Smitt PAES *et al.* A proteome comparison between physiological angiogenesis and angiogenesis in glioblastoma. *Mol Cell Proteomics* 2012; **11**: M111.008466.
29 Riabov V, Gudima A, Wang N, Mickley A, Orekhov A, Kzhyshkowska J. Role of tumor associated macrophages in tumor angiogenesis and lymphangiogenesis. *Front Physiol* 2014; **5**: 75.
30 Armulik A, Genove G, Betsholtz C. Pericytes: developmental, physiological, and pathological perspectives, problems, and promises. *Dev Cell* 2011; **21**: 193–215.
31 Sweeney MD, Ayyadurai S, Zlokovic BV. Pericytes of the neurovascular unit: key functions and signaling pathways. *Nat Neurosci* 2016; **19**: 771–783.
32 Bergers G, Song S. The role of pericytes in blood-vessel formation and maintenance. *Neuro Oncol* 2005; **7**: 452–464.
33 Garcia-Quintans N, Sanchez-Ramos C, Prieto I, Tierrez A, Arza E, Alfranca A *et al.* Oxidative stress induces loss of pericyte coverage and vascular instability in PGC-1 alpha-deficient mice. *Angiogenesis* 2016; **19**: 217–228.
34 Stark K, Eckart A, Haidari S, Tirniceriu A, Lorenz M, von Bruhl M-L *et al.* Capillary and arteriolar pericytes attract innate leukocytes exiting through venules and 'instruct' them with pattern-recognition and motility programs. *Nat Immunol* 2013; **14**: 41–51.
35 Yang YL, Andersson P, Hosaka K, Zhang Y, Cao RH, Iwamoto H *et al.* The PDGF-BB-SOX7 axis-modulated IL-33 in pericytes and stromal cells promotes metastasis through tumour-associated macrophages. *Nat Commun* 2016; **7**: 11385.
36 Yang L, DeBusk LM, Fukuda K, Fingleton B, Green-Jarvis B, Shyr Y *et al.* Expansion of myeloid immune suppressor Gr+CD11b+cells in tumor-bearing host directly promotes tumor angiogenesis. *Cancer Cell* 2004; **6**: 409–421.
37 Zhu C, van der Weiden MM, Scchetti A, van den Bosch TPP, Chrifi I, Brandt MM *et al.* Abstract 2348: expression of CECR1 by activated M2-type macrophages in glioma. *Cancer Res* 2015; **75**(15 Supplement): 2348.
38 Vignaud JM, Marie B, Klein N, Plenat F, Pech M, Borrelly J *et al.* The role of platelet-derived growth-factor production by tumor-associated macrophages in tumor stroma formation in lung cancer. *Cancer Res* 1994; **54**: 5455–5463.
39 Xue Y, Lim S, Yang Y, Wang Z, Jensen LD, Hedlund EM *et al.* PDGF-BB modulates hematopoiesis and tumor angiogenesis by inducing erythropoietin production in stromal cells. *Nat Med* 2012; **18**: 100–110.
40 Sun HQ, Guo DY, Su YP, Yu DM, Wang QL, Wang T *et al.* Hyperplasia of pericytes is one of the main characteristics of microvascular architecture in malignant glioma. *PLoS One* 2014; **9**: e114246.
41 Ochs K, Sahm F, Opitz CA, Lanz TV, Oezen I, Couraud PO *et al.* Immature mesenchymal stem cell-like pericytes as mediators of immunosuppression in human malignant glioma. *J Neuroimmunol* 2013; **265**: 106–116.
42 Zhong X, Liu X, Li Y, Cheng M, Wang W, Tian K *et al.* HMGA2 sustains self-renewal and invasiveness of glioma-initiating cells. *Oncotarget* 2016; **7**: 44365–44380.
43 Liu AY, Zheng H, Ouyang G. Periostin, a multifunctional matricellular protein in inflammatory and tumor microenvironments. *Matrix Biol* 2014; **37**: 150–156.
44 Park SY, Piao Y, Jeong KJ, Dong J, de Groot JF. Periostin (POSTN) regulates tumor resistance to antiangiogenic therapy in glioma models. *Mol Cancer Ther* 2016; **15**: 2187–2197.
45 Malanchi I, Santamaria-Martinez A, Susanto E, Peng H, Lehr HA, Delaloye JF *et al.* Interactions between cancer stem cells and their niche govern metastatic colonization. *Nature* 2012; **481**: 85–U95.
46 Erkan M, Kleeff J, Gorbachevski A, Reiser C, Mitkus T, Esposito I *et al.* Periostin creates a tumor-supportive microenvironment in the pancreas by sustaining fibrogenic stellate cell activity. *Gastroenterology* 2007; **132**: 1447–1464.
47 Zheng PP, van der Weiden M, Kros JM. Fast tracking of co-localization of multiple markers by using the nanozoomer slide scanner and NDPViewer. *J Cell Physiol* 2014; **229**: 967–973.
48 Koh W, Stratman AN, Sacharidou A, Davis GE. *In vitro* three dimensional collagen matrix models of endothelial lumen formation during vasculogenesis and angiogenesis. *Methods Enzymol* 2008; **443**: 83–101.

Supplementary Information accompanies this paper on the Oncogene website (http://www.nature.com/onc)